Available online at www.sciencedirect.com
SCIENCE DIRECT®
Engineering Failure Analysis 13 (2006) 629–637
ENGINEERING FAILURE ANALYSIS
www.elsevier.com/locate/engfailanal

A numerical analysis of stress intensity factors at bifurcated cracks

Xiangqiao Yan

Research Laboratory on Composite Materials, Harbin Institute of Technology, Harbin 150001, PR China

Received 28 October 2004; accepted 11 December 2004
Available online 22 April 2005

Abstract

This paper is concerned with complex stress intensity factors at bifurcated cracks by using the boundary element method, which consists of the constant displacement discontinuity element presented by Crouch and Starfield and the crack-tip displacement discontinuity element due to the author. To prove the efficiency of the suggested approach and provide more results of the stress intensity factors, analysis of an asymmetric branched crack bifurcated from a main crack is carried out. The present numerical results show that the numerical approach to the computation of stress intensity factors of complex plane crack problems is simple, yet very accurate.

Keywords: Stress intensity factor; Boundary element method; Displacement discontinuity; Crack; Crack-tip element

1. Introduction

Stress intensity factors are important in the analysis of cracked materials. They are directly related to the fracture propagation and fatigue crack growth criteria. In the beginning, the majority of the analyses of crack problems were mostly based on the Muskhelishvili potential formulation and conformal mapping of the crack geometry. With the development of numerical computational techniques, in recent years, numerical analysis methods, in particular, finite element method and boundary element method are used extensively in solving the crack problems. It is well known that how to model the crack is the key issue in the analyses. Among several elastic two-dimensional crack modeling strategies by the boundary element method, there exist the multi-domain formulation [1], the stress formulation with regularization [2], and the dual boundary element method [3,4]. For each formulation, options are available such as building in the

E-mail address: Yanxiangqiao@hotmail.com

1350-6307/$ - see front matter
doi:10.1016/j.engfailanal.2004.12.043

crack-tip stress singularity [5], using the quarter-point boundary element [1], and strategically refining the near-crack-tip nonsingular element. Further details of elastic crack analysis by the boundary element method are given in [6,7].

Even though much progress has been made in crack modeling techniques, both simple and very accurate crack modeling technique is still needed, in particular for the branched crack problems. The displacement discontinuity method [8], as an indirect boundary element method, is very well suited for analysis the crack problems in plane elasticity because, physically, one may imagine a displacement discontinuity as a line crack whose opposing surfaces have been displaced relative to one another. Based on the analytical solution [8,9] to the problem of a constant discontinuity in displacement over a finite line segment in the x, y plane of an infinite elastic solid, recently, the crack-tip displacement discontinuity element, which can be classified as the left and right crack-tip displacement discontinuity elements were presented by the author [10] to model the crack-tip fields to very accurately compute the stress intensity factors of cracks in general plane elasticity. In [11], the crack-tip displacement discontinuity element together with the constant displacement discontinuity element presented by Crouch and Starfield [8] is used to develop a numerical approach to the computation of stress intensity factors of plane elasticity cracks. In the boundary element implementation, the left or the right crack-tip element is placed locally at the corresponding left or right crack tip on top of the constant displacement discontinuity elements that cover the entire crack surface and the other boundaries. To prove the efficiency of the suggested approach and provide more results of the stress intensity factors, analysis of an asymmetric branched crack bifurcated from a main crack is carried out. The problem was ever analyzed by Theocaris [12] by optical method and documented by Murakkami [13]. The present numerical results show that the numerical approach to the computation of stress intensity factors of complex plane crack problems is simple, yet very accurate.

2. Numerical procedure

A boundary element method proposed in [11] for calculating numerically stress intensity factors for plane elasticity crack problems consists of the constant displacement discontinuity element presented by Crouch and Starfield [8] and the crack-tip displacement discontinuity element due to the author [10].

2.1. Brief introduction of constant displacement discontinuity element [8]

The displacement discontinuity D_i in $|x| < a$, $y = 0$ in an infinite plate is defined as the difference in displacement between the two sides of the segment [8]:

$$\begin{aligned} D_x &= u_x(x,0_-) - u_x(x,0_+), \\ D_y &= u_y(x,0_-) - u_y(x,0_+). \end{aligned} \tag{1}$$

Because u_x and u_y are positive in the positive x and y coordinate directions, it follows that D_x and D_y are positive as illustrated in Fig. 1.

The solution to the subject problem is given by Crouch and Starfield [8]. The displacements and stresses can be written as

$$\begin{aligned} u_x &= D_x[2(1-v)F_3(x,y) - yF_5(x,y)] + D_y[-(1-2v)F_2(x,y) - yF_4(x,y)], \\ u_y &= D_x[(1-2v)F_2(x,y) - yF_4(x,y)] + D_y[2(1-v)F_3(x,y) - yF_5(x,y)] \end{aligned} \tag{2}$$

and

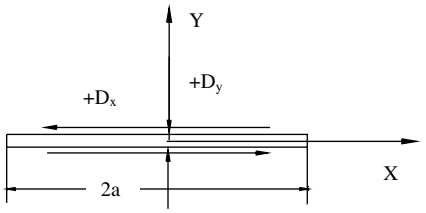

Fig. 1. Schematic of constant displacement discontinuity components D_x and D_y.

$$\begin{aligned}
\sigma_{xx} &= 2GD_x[2F_4(x,y) + yF_6(x,y)] + 2GD_y[-F_5(x,y) + yF_7(x,y)],\\
\sigma_{yy} &= 2GD_x[-yF_6(x,y)] + 2GD_y[-F_5(x,y) - yF_7(x,y)],\\
\sigma_{xy} &= 2GD_x[-F_5(x,y) + yF_7(x,y)] + 2GD_y[-yF_6(x,y)].
\end{aligned} \tag{3}$$

G and v in these equations are shear modulus and the Poisson's ratio, respectively. Functions F_2 through F_7 are described in [8]. Eqs. (2) and (3) are used by Crouch and Starfield [8] to set up a constant displacement discontinuity boundary element method.

2.2. Crack-tip displacement discontinuity element

Based on [8], the crack-tip displacement discontinuity elements, which can be classified as the left and the right crack-tip displacement discontinuity element to deal with crack problems for general plane elasticity, were presented by the author [10]. The left crack-tip displacement discontinuity element is outlined here.

The schematic of the left crack-tip displacement discontinuity element is shown in Fig. 2. Its displacement discontinuity functions are chosen as

$$\begin{aligned}
\boldsymbol{D_x} &= \boldsymbol{H}_{\mathrm{s}}\left(\frac{\boldsymbol{a}+\xi}{\boldsymbol{a}}\right)^{\frac{1}{2}},\\
\boldsymbol{D_y} &= \boldsymbol{H}_{\mathrm{n}}\left(\frac{\boldsymbol{a}+\xi}{\boldsymbol{a}}\right)^{\frac{1}{2}},
\end{aligned} \tag{4}$$

where H_{s} and H_{n} are the tangential and normal displacement discontinuity quantities at the center of the element, respectively. Here, it is noted that the element has the same unknowns as the two-dimensional constant displacement discontinuity element. But it can be seen that the displacement discontinuity functions

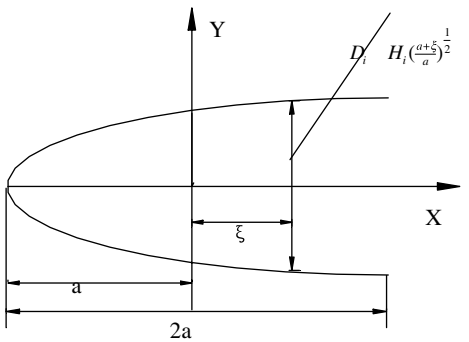

Fig. 2. Schematic of the left crack-tip displacement discontinuity element.

defined according to (4) can model the displacement fields around the crack tip. Therefore, the stress field determined by the displacement discontinuity functions (4) possesses the $r^{-1/2}$ singularity around the crack tip.

Based on the solution of constant discontinuity in displacement given by Crouch and Starfield [8], the displacements and stresses at a point (x, y) due to the left crack-tip displacement discontinuity element can be obtained as follows:

$$\begin{aligned} u_x &= H_s[2(1-v)B_3(x,y) - yB_5(x,y)] + H_n[-(1-2v)B_2(x,y) - yB_4(x,y)], \\ u_y &= H_s[(1-2v)B_2(x,y) - yB_4(x,y)] + H_n[2(1-v)B_3(x,y) - yB_5(x,y)] \end{aligned} \tag{5}$$

and

$$\begin{aligned} \sigma_{xx} &= 2GH_s[2B_4(x,y) + yB_6(x,y)] + 2GH_n[-B_5(x,y) + yB_7(x,y)], \\ \sigma_{yy} &= 2GH_s[-yB_6(x,y)] + 2GH_n[-B_5(x,y) - yB_7(x,y)], \\ \sigma_{xy} &= 2GH_s[-B_5(x,y) + yB_7(x,y)] + 2GH_n[-yB_6(x,y)], \end{aligned} \tag{6}$$

where functions B_2 through B_7 are given in [10].

It can be seen by comparing Eqs. (5) and (6) with Eqs. (2) and (3) that the displacements and stresses due to the crack-tip displacement discontinuity element possess the same forms as those due to a constant displacement discontinuity element, with $F_i(x, y)$ $(i = 2, 3, \ldots, 7)$ in Eqs. (2) and (3) being replaced by $B_i(x, y)$ $(i = 2, 3, \ldots, 7)$, D_x and D_y by H_s and H_n, respectively. This enables the boundary element implementation to be easy.

3. Computation formulas of stress intensity factors and simple illustrative examples

Based on the displacement field around the crack tip and the definition of the displacement discontinuity functions (11), one can obtain the calculation formulas of stress intensity factors K_I and K_{II}:

$$K_I = -\frac{\sqrt{2\pi}GH_n}{4(1-v)\sqrt{a}}, \quad K_{II} = -\frac{\sqrt{2\pi}GH_s}{4(1-v)\sqrt{a}}. \tag{7}$$

To prove the efficiency of the suggested approach, two simple illustrative examples are taken here.

An infinite plate with a through crack of length $2a$ which is subjected to uniform stress normal to the crack plane at distances sufficiently far away from the crack is taken for example to compute the stress intensity factor K_I. Owing to its symmetry, only half is taken for the analysis. Table 1 gives that the ratio of the numerical solution to the analytical one for stress intensity factor K_I is varied with the number of elements. In this calculation, the crack-tip element and constant elements are taken to possess the equal size. Table 2 gives that the ratio of the numerical solution to the analytical one for stress intensity factor K_I is varied with the ratio of the size of the crack-tip element to the one of constant elements. Here, the sizes of constant elements are taken to be equal and the number of total elements is 11. It can be seen from Table 1 that a good result for the stress intensity factor K_I can be obtained using the crack-tip element. It can be seen from Table 2 that the ratio of the size of the crack-tip element to that of constant elements is

Table 1
Variation of SIF normalized by $\sigma\sqrt{\pi a}$ for a center crack in an infinite plate with the number of elements

Number of elements	3	5	7	10	15	25
$K_I/\sigma\sqrt{\pi a}$	0.9621	0.9775	0.9838	0.9885	0.9921	0.995

Table 2
Variation of SIF normalized by $\sigma\sqrt{\pi a}$ for a center crack in an infinite plate with the ratio of the size of the crack-tip element to the one of constant elements

$a_{crack}/a_{constant}$	0.60	0.65	0.70	0.75	0.80	0.85	0.90	0.95	1.00
$K_I/\sigma\sqrt{\pi a}$	1.2048	1.1690	1.1394	1.1143	1.0928	1.0742	1.0578	1.0433	1.0303
$a_{crack}/a_{constant}$	1.05	1.10	1.15	1.20	1.25	1.30	1.35	1.40	1.45
$K_I/\sigma\sqrt{\pi a}$	1.0186	1.0080	0.9984	0.9896	0.9815	0.9741	0.9671	0.9607	0.9547

Table 3
Variation of normalized SIF s for an inclined center crack in an infinite plate with the angle β

β	5°	10°	20°	30°	40°	45°	50°	60°	70°	80°	85°
F_I	0.9895	0.9898	0.9896	0.9898	0.9898	0.9885	0.9897	0.9897	0.9898	0.9897	0.9896
F_{II}	0.9896	0.9897	0.9897	0.9897	0.9897	0.9885	0.9897	0.9897	0.9897	0.9897	0.9896

necessarily taken to be from 0.9 to 1.3 to obtain a good result with a relative error less than 3%. This can be regarded as one limitation to the approach presented in the present paper.

An inclined crack plate with a through crack of length $2a$ which is subjected to uniform stress at distances sufficiently far away from the crack is taken as another example to compute the SIFs K_I and K_{II} whose exact solution is available [13]. Here, the SIFs K_I and K_{II} calculated by the present study are normalized by

$$F_I = K_I/(\sigma\sqrt{\pi a}\sin^2\beta), \quad F_{II} = K_{II}/(\sigma\sqrt{\pi a}\sin\beta\cos\beta),$$

where β is the angle between the load and the crack plane. Some numerical results are given in Table 3. In this calculation, the crack-tip elements and constant elements are taken to be of equal size and the number of total elements is taken to be 20, i.e., two crack-tip elements and 18 constant elements. It is observed from Table 3 that no matter how large or small is the angle β between the load and the crack plane, the present numerical results of the stress intensity factors K_I and K_{II} are in good agreement with the analytical ones.

4. Stress intensity factors for an asymmetric branched crack bifurcated from main crack

To prove further the efficiency of the suggested approach and provide more results of the stress intensity factors, analysis of an asymmetric branched crack bifurcated from a main crack is carried out below. The

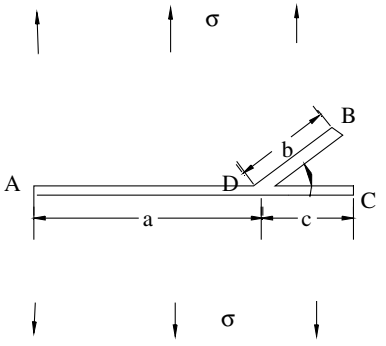

Fig. 3. Schematic of an asymmetric branched crack under uniaxial tension.

Table 4
Variation of the number of elements discretized on segments AD, DB and DC with ratios c/a and b/c

b/c	c/a											
	0.1			0.15			0.2			0.25		
	n_a	n_b	n_c	n_a	n_b	n_c	n_a	n_b	n_c	n_a	n_b	n_c
0.2	500	10	50	333	10	50	250	10	50	200	10	50
0.4	250	10	25	166	10	25	187	15	37	200	20	50
0.6	160	10	16	222	20	33	166	20	33	133	20	33
0.8	180	15	18	166	20	25	125	25	25	100	20	25
1.0	200	20	20	166	25	25	125	30	25	100	25	25
1.2	200	24	20	166	30	25	125	35	25	100	30	25
1.4	200	28	20	166	35	25	125	40	25	100	35	25
1.6	200	32	20	166	40	25	125	45	25	100	40	25
1.8	200	36	20	166	45	25	125	50	25	100	45	25
2.0	200	40	20	166	50	25	125	55	25	100	50	25
2.2	200	44	20	166	55	25	125	55	25	100	55	25
2.4	200	48	20	166	60	25	125	60	25	100	60	25
2.6	200	52	20	166	65	25	125	65	25	100	65	25
2.8	200	56	20	166	70	25	125	70	25	100	70	25
3.0	200	60	20	166	75	25	125	75	25	100	75	25

Table 5
Normalized stress intensity factors for an asymmetric branching crack angle $\theta = 15°$

b/c	$c/a = 0.10$				$c/a = 0.15$			
	$F_{\mathrm{I}}^{\mathrm{B}}$	$F_{\mathrm{II}}^{\mathrm{B}}$	$F_{\mathrm{I}}^{\mathrm{C}}$	$F_{\mathrm{II}}^{\mathrm{C}}$	$F_{\mathrm{I}}^{\mathrm{B}}$	$F_{\mathrm{II}}^{\mathrm{B}}$	$F_{\mathrm{I}}^{\mathrm{C}}$	$F_{\mathrm{II}}^{\mathrm{C}}$
0.2	−0.0468	0.0579	0.9959	−0.0033	−0.0538	0.0656	0.996	−0.0035
0.4	−0.0563	0.0701	0.9937	−0.0105	−0.0663	0.0803	0.9935	−0.0114
0.6	−0.0164	0.0665	1.0003	−0.0098	−0.0398	0.0476	0.9973	−0.0181
0.8	0.1433	−0.0199	0.9913	0.0042	0.1213	−0.0288	0.9899	−0.0134
1.0	0.616	−0.0231	0.7735	0.1206	0.6146	−0.0147	0.7823	0.1152
1.2	0.9014	0.1457	0.3645	0.1496	0.9048	0.1602	0.3666	0.1455
1.4	0.9538	0.2127	0.165	0.0888	0.9596	0.2285	0.1618	0.0833
1.6	0.9685	0.234	0.0819	0.0446	0.9774	0.2506	0.0755	0.0376
1.8	0.9777	0.2439	0.0402	0.0169	0.9897	0.2612	0.0318	0.0087
2.0	0.9857	0.2503	0.0156	−0.0015	1.0011	0.2682	0.0058	−0.0107
	$c/a = 0.20$				$c/a = 0.25$			
	$F_{\mathrm{I}}^{\mathrm{B}}$	$F_{\mathrm{II}}^{\mathrm{B}}$	$F_{\mathrm{I}}^{\mathrm{C}}$	$F_{\mathrm{II}}^{\mathrm{C}}$	$F_{\mathrm{I}}^{\mathrm{B}}$	$F_{\mathrm{II}}^{\mathrm{B}}$	$F_{\mathrm{I}}^{\mathrm{C}}$	$F_{\mathrm{II}}^{\mathrm{C}}$
0.2	−0.0599	0.0708	0.996	−0.0036	−0.0644	0.0754	0.9959	−0.0037
0.4	−0.0717	0.0806	0.9957	−0.0086	−0.0806	0.0796	0.9965	−0.0097
0.6	−0.0499	0.0564	0.9976	−0.0205	−0.0581	0.0632	0.9978	−0.0224
0.8	0.1125	−0.0199	0.9918	−0.0187	0.1055	−0.013	0.9933	−0.0231
1.0	0.612	−0.0047	0.7865	0.1086	0.6102	0.003	0.7899	0.1033
1.2	0.9071	0.1727	0.3665	0.1399	0.9094	0.1823	0.3664	0.1353
1.4	0.9647	0.2415	0.1578	0.0768	0.9696	0.2515	0.1542	0.0715
1.6	0.9853	0.2638	0.0691	0.03	0.9929	0.2739	0.0637	0.0239
1.8	1.0007	0.2745	0.0238	0.0003	1.011	0.2848	0.0171	−0.0066
2.0	1.015	0.2819	−0.0032	−0.0198	1.028	0.2924	−0.0108	−0.0272

problem was ever analyzed by Theocaris [12] by optical method and documented by Murakkami [13]. The schematic of the asymmetric branched crack is shown in Fig. 3. In the present analysis, the following cases are considered

$$c/a = 0.1, 0.15, 0.20, 0.25,$$

$$\theta = 15^\circ, \quad b/c = 0.2, 0.4, 0.6, 0.8, 1.0, 1.2, 1.4, 1.6, 1.8, 2.0,$$

$$\theta = 30^\circ, \quad b/c = 0.2, 0.4, 0.6, 0.8, 1.0, 1.2, 1.4, 1.6, 1.8, 2.0,$$

$$\theta = 45^\circ, \quad b/c = 0.2, 0.4, 0.6, 0.8, 1.0, 1.2, 1.4, 1.6, 1.8, 2.0, 2.2, 2.4, 2.6, 2.8, 3.0.$$

The stress intensity factors at the crack tips B and C are normalized by mode-I stress intensity factors at the crack tip A, i.e.,

$$F_{\mathrm{IB}} = K_{\mathrm{IB}}/K_{\mathrm{IA}}, \quad F_{\mathrm{IIB}} = K_{\mathrm{IIB}}/K_{\mathrm{IA}},$$

$$F_{\mathrm{IC}} = K_{\mathrm{IC}}/K_{\mathrm{IA}}, \quad F_{\mathrm{IIC}} = K_{\mathrm{IIC}}/K_{\mathrm{IA}}.$$

Regarding the discretization of boundary elements, here, the number of elements discretized on segments AD, DB and DC is denoted by n_a n_b and n_c, respectively, and is varied with ratios c/a and b/c, as listed in Table 4. Stress intensity factors for the branched crack angles 15°, 30° and 45° are given in Tables 5–7. If the reader compares the numerical results here with those reported in [12], it is found that the consistency between the two is very good in tendency. But because the results reported in [12] were represented by curves,

Table 6
Normalized stress intensity factors for an asymmetric branching crack angle $\theta = 30^\circ$

b/c	$c/a = 0.10$				$c/a = 0.15$			
	$F_{\mathrm{I}}^{\mathrm{B}}$	$F_{\mathrm{II}}^{\mathrm{B}}$	$F_{\mathrm{I}}^{\mathrm{C}}$	$F_{\mathrm{II}}^{\mathrm{C}}$	$F_{\mathrm{I}}^{\mathrm{B}}$	$F_{\mathrm{II}}^{\mathrm{B}}$	$F_{\mathrm{I}}^{\mathrm{C}}$	$F_{\mathrm{II}}^{\mathrm{C}}$
0.2	−0.0722	0.0617	0.9975	−0.0033	−0.0881	0.0734	0.9976	−0.0038
0.4	−0.064	0.0615	0.9979	−0.0119	−0.0847	0.077	0.998	−0.0145
0.6	0.0236	0.0373	0.9989	−0.0165	−0.0006	0.0431	1.0023	−0.0233
0.8	0.2356	0.0204	0.9759	0.0126	0.2163	0.0337	0.9824	0.0004
1.0	0.5057	0.0913	0.8641	0.0852	0.4928	0.1106	0.8744	0.0729
1.2	0.6847	0.21	0.6838	0.139	0.677	0.2342	0.6929	0.1282
1.4	0.7656	0.3016	0.5204	0.1485	0.7612	0.329	0.5256	0.1387
1.6	0.8	0.3587	0.4013	0.136	0.7983	0.3884	0.4022	0.1262
1.8	0.8165	0.3947	0.3176	0.1178	0.8176	0.426	0.3148	0.1074
2.0	0.8262	0.4191	0.2574	0.0997	0.8301	0.4517	0.2514	0.0887
	$c/a = 0.20$				$c/a = 0.25$			
	$F_{\mathrm{I}}^{\mathrm{B}}$	$F_{\mathrm{II}}^{\mathrm{B}}$	$F_{\mathrm{I}}^{\mathrm{C}}$	$F_{\mathrm{II}}^{\mathrm{C}}$	$F_{\mathrm{I}}^{\mathrm{B}}$	$F_{\mathrm{II}}^{\mathrm{B}}$	$F_{\mathrm{I}}^{\mathrm{C}}$	$F_{\mathrm{II}}^{\mathrm{C}}$
0.2	−0.1004	0.0824	0.9975	−0.0043	−0.1103	0.0898	0.9974	−0.0047
0.4	−0.1032	0.0836	0.9991	−0.0158	−0.1175	0.0904	0.9998	−0.0175
0.6	−0.0179	0.0558	1.0037	−0.0286	−0.0317	0.0656	1.0048	−0.033
0.8	0.2018	0.047	0.9864	−0.0083	0.1905	0.0571	0.9896	−0.0153
1.0	0.4834	0.1259	0.8806	0.0633	0.4766	0.1374	0.8854	0.0556
1.2	0.6719	0.2522	0.6981	0.1195	0.669	0.2659	0.7018	0.1125
1.4	0.7594	0.3493	0.5277	0.1306	0.7593	0.3646	0.529	0.124
1.6	0.7993	0.4101	0.4011	0.118	0.8018	0.4266	0.3997	0.1113
1.8	0.8212	0.4487	0.3109	0.0987	0.8261	0.466	0.3071	0.0916
2.0	0.8363	0.4753	0.2451	0.0793	0.8435	0.4932	0.2394	0.0716

Table 7
Normalized stress intensity factors for an asymmetric branching crack angle $\theta = 45°$

b/c	$c/a = 0.10$				$c/a = 0.15$			
	F_I^B	F_{II}^B	F_I^C	F_{II}^C	F_I^B	F_{II}^B	F_I^C	F_{II}^C
0.2	−0.1343	0.0382	1.0005	−0.0047	−0.1621	0.048	1.0009	−0.0057
0.4	−0.1208	0.0313	1.0056	−0.0192	−0.1564	0.0435	1.0067	−0.024
0.6	−0.0113	0.0337	1.0116	−0.0306	−0.0317	0.0542	1.0121	−0.0364
0.8	0.1685	0.0772	0.9967	−0.013	0.138	0.0936	1.0038	−0.0273
1.0	0.3345	0.1603	0.945	0.0258	0.3103	0.183	0.9547	0.0112
1.2	0.4514	0.2583	0.8612	0.0672	0.4305	0.2844	0.8721	0.0525
1.4	0.5191	0.3422	0.7694	0.0953	0.501	0.3714	0.7797	0.081
1.6	0.5559	0.4062	0.685	0.1097	0.5404	0.438	0.6935	0.0959
1.8	0.576	0.4541	0.6128	0.115	0.563	0.488	0.6189	0.1014
2.0	0.5874	0.4903	0.5523	0.1149	0.5769	0.526	0.556	0.1012
2.2	0.5944	0.5187	0.5017	0.1118	0.5862	0.5557	0.503	0.0979
2.4	0.5989	0.5415	0.4591	0.1072	0.5932	0.5798	0.458	0.0929
2.6	0.6023	0.5605	0.4227	0.1018	0.599	0.5999	0.4194	0.0871
2.8	0.6049	0.5768	0.3913	0.0961	0.6041	0.6171	0.386	0.0809
3.0	0.6073	0.5909	0.3638	0.0903	0.6088	0.6321	0.3567	0.0746
	$c/a = 0.20$				$c/a = 0.25$			
	F_I^B	F_{II}^B	F_I^C	F_{II}^C	F_I^B	F_{II}^B	F_I^C	F_{II}^C
.2	−0.1837	0.0554	1.0011	−0.0066	−0.2007	0.0618	1.0011	−0.0074
.4	−0.1691	0.0604	1.0065	−0.0264	−0.1827	0.0723	1.0063	−0.0286
.6	−0.0583	0.0648	1.0149	−0.0446	−0.0792	0.0726	1.0171	−0.0513
.8	0.1145	0.1053	1.0097	−0.0393	0.0968	0.1136	1.0143	−0.0491
1.0	0.2914	0.1971	0.9631	−0.0024	0.2779	0.2072	0.9695	−0.0133
1.2	0.4157	0.3013	0.8812	0.0389	0.4059	0.3134	0.888	0.028
1.4	0.4896	0.3907	0.788	0.0679	0.4827	0.4047	0.7939	0.0575
1.6	0.5318	0.4594	0.7002	0.0833	0.5275	0.4748	0.7047	0.0732
1.8	0.5569	0.5109	0.6236	0.089	0.5549	0.5273	0.6265	0.079
2.0	0.5732	0.55	0.5587	0.0887	0.5733	0.5674	0.5599	0.0787
2.2	0.5849	0.5808	0.5037	0.0853	0.5869	0.5989	0.5033	0.0751
2.4	0.5941	0.6057	0.4569	0.08	0.5981	0.6244	0.4549	0.0696
2.6	0.602	0.6265	0.4166	0.0738	0.6078	0.6458	0.4131	0.0631
2.8	0.6091	0.6443	0.3815	0.0672	0.6167	0.6641	0.3767	0.0562
3.0	0.6159	0.6599	0.3507	0.0605	0.6251	0.6801	0.3445	0.0492

the quantitative comparisons cannot be made here. It can be seen from the curves of the normalized stress intensity factors given in [12] and the present numerical results that the effect of the ratio b/c on the normalized stress intensity factors is very obvious, especially for F_{IB}, F_{IIB} and F_{IC}. However, the effect of the ratio c/a on the normalized stress intensity factors F_{IB}, F_{IIB}, F_{IC} and F_{IIC} is not revealed from the curves of the normalized stress intensity factors given in [12]. In fact, it can be seen from the present numerical results, see Tables 5–7, that the ratio c/a affects also the normalized stress intensity factors F_{IB}, F_{IIB}, F_{IC} and F_{IIC}. For example, for the case, $\theta = 15°$, $b/c = 0.2$, F_{IB} and F_{IIB} corresponding to $c/a = 0.1$, 0.15, 0.2, 0.25 are −0.0468, −0.0538, −0.0599, −0.0644, and 0.0579, 0.0656, 0.0708, 0.0754, respectively; on the other hand, F_{IC} and F_{IIC} corresponding to $c/a = 0.1$, 0.15, 0.2, 0.25 are 0.9959, 0.9960, 0.9960, 0.9959 and −0.0033, −0.0035, −0.0036, −0.0038, respectively. For this case, apparently, the effect of the ratio c/a on F_{IB} and F_{IIB} is very obvious, but the effect of the ratio c/a on F_{IC} and F_{IIC} is almost negligible. For example again, for the case, $\theta = 30°$, $b/c = 2.0$, the ratio c/a has an effect on F_{IB}, F_{IIB}, F_{IC}, F_{IIC} to some extent.

5. Conclusion

This paper studies complex stress intensity factors at bifurcated cracks by using a boundary element method. The present numerical results show that the numerical approach to the computation of stress intensity factors of complex plane crack problems is simple, yet very accurate.

Acknowledgement

Special thanks are due to the National Natural Science Foundation of China (No: 10272037) for supporting the present work.

References

[1] Blandford GE, Ingraffea AR, Liggett JA. Two-dimensional stress intensity factor computations using the boundary element method. Int J Num Meth Eng 1981;17:387–404.
[2] Balas J, Sladek J, Sladek V. Stress analysis by boundary element methods. Amsterdam: Elsevier; 1989.
[3] Hong H, Chen J. Derivatives of integral equations of elasticity. J Eng Mech 1988;114(6):1028–44.
[4] Portela A, Aliabadi MH. The dual boundary element method: effective implementation for crack problems. Int J Num Meth Eng 1992;33:1269–87.
[5] Tanaka M, Itoh H. New crack elements for boundary element analysis of elastostatics considering arbitrary stress singularities. Appl Math Model 1987;11:357–63.
[6] Cruse TA. Boundary element analysis in computational fracture mechanics. Dordrecht: Kluwer; 1989.
[7] Aliabadi MH, Rooke DP. Numerical fracture mechanics. Southampton: Computational Mechanics Publications and Dordrecht: Kluwer; 1991.
[8] Crouch SL, Starfield AM. Boundary element method in solid mechanics, with application in rock mechanics and geological mechanics, London, Geore Allon & Unwin, Bonton, Sydney; 1983.
[9] Crouch SL. Solution of plane elasticity problems by displacement discontinuity method. Int J Num Meth Eng 1976;10:301–43.
[10] Yan X. A Crack tip displacement discontinuity element. Mech Res Commun 2004;31(6):651–9.
[11] Yan X. Stress intensity factors for cracks emanating from a triangular or square hole in an infinite plate by boundary elements. Eng Fail Anal 2005;12(3):362–75.
[12] Theocaris PS. Complex stress intensity factors at bifurcated crack. J Mech Phys Solids 1972;20:265–79.
[13] Murakami Y. Stress intensity factors handbook. New York: Pergamon Press; 1987.